European Journal of Pharmaceutical Sciences 98 (2017) 4–16

Contents lists available at ScienceDirect

European Journal of Pharmaceutical Sciences

journal homepage: www.elsevier.com/locate/ejps

Biological reference materials for extracellular vesicle studies

S. Valkonen [a,b,*], E. van der Pol [c,d], A. Böing [c], Y. Yuana [c], M. Yliperttula [e,f], R. Nieuwland [c], S. Laitinen [b], P.R.M. Siljander [a]

[a] EV Group, Biochemistry and Biotechnology, Faculty of Biological and Environmental Sciences, Division of Pharmaceutical Biosciences, Faculty of Pharmacy, University of Helsinki, Finland
[b] Finnish Red Cross Blood Service, Helsinki, Finland
[c] Department of Clinical Chemistry, Academic Medical Center, University of Amsterdam, The Netherlands
[d] Department of Biomedical Engineering and Physics, Academic Medical Center, University of Amsterdam, The Netherlands
[e] Division of Pharmaceutical Biosciences, Faculty of Pharmacy, University of Helsinki, Finland
[f] Department of Pharmaceutical and Pharmacological Sciences, University of Padova, Italy

ARTICLE INFO

Article history:
Received 13 May 2016
Received in revised form 6 September 2016
Accepted 6 September 2016
Available online 10 September 2016

Keywords:
Extracellular vesicles
Nanoerythrosome
Reference material
Standardization
Characterization
Quantification

ABSTRACT

Extracellular vesicles (EVs) mediate normal physiological homeostasis and pathological processes by facilitating intercellular communication. Research of EVs in basic science and clinical settings requires both methodological standardization and development of reference materials (RM). Here, we show insights and results of biological RM development for EV studies. We used a three-step approach to find and develop a biological RM. First, a literature search was done to find candidates for biological RMs. Second, a questionnaire was sent to EV researchers querying the preferences for RM and their use. Third, a biological RM was selected, developed, characterized, and evaluated.

The responses to the survey demonstrated a clear and recognized need for RM optimized for the calibration of EV measurements. Based on the literature, naturally occurring and produced biological RM, such as virus particles and liposomes, were proposed as RM. However, none of these candidate RMs have properties completely matching those of EVs, such as size and refractive index distribution. Therefore, we evaluated the use of nanoerythrosomes (NanoE), vesicles produced from erythrocytes, as a potential biological RM. The strength of NanoE is their resemblance to EVs. Compared to the erythrocyte-derived EVs (eryEVs), NanoE have similar morphology, a similar refractive index (1.37), larger diameter (70% of the NanoE are over 200 nm), and increased positive staining for CD235a and lipids (Di-8-ANEPPS) (58% and 67% in NanoE vs. 21% and 45% in eryEVs, respectively).

Altogether, our results highlight the general need to develop and validate new RM with similar physical and biochemical properties as EVs to standardize EV measurements between instruments and laboratories.

1. Introduction

Extracellular vesicles (EVs) are lipid bilayer surrounded particles that contain proteins, lipids, metabolites, and nucleic acids (Yanez-Mo et al., 2015). EVs are produced by most cells, including bacteria and plant cells, making cross-kingdom communication possible (Samuel et al., 2015). EVs have active physiological and pathophysiological roles and they are functional components of intercellular communication, thereby offering possibilities in the development of therapy and diagnostics, or collectively, theranostics (Fais et al., 2016). EVs are often classified into exosomes and microvesicles based on size and the route of formation, but increasing data have revealed this to be an oversimplification, since the isolated populations are heterogeneous and have overlapping properties including size, density, and molecular markers (van der Pol et al., 2016).

The molecular content and concentrations of EVs in human body fluids have raised increasing interest for their use as biomarkers (Fais et al., 2016). A biomarker based on EVs has not yet been realized, partly due to the lack of standardization. Standardization is difficult because the calibration of instruments, the interpretation and validation of results, and the comparison of measurements require a reference material (RM) with physical properties equal to EVs. One of the most analyzed property of an EV sample is the concentration. However, the measured EV concentration depends on the physical properties of EVs, such as the size distribution and refractive index (RI), complicating the analysis, as explained below.

EVs smaller than 300 nm constitute the majority of EV population (Aatonen et al., 2014; Arraud et al., 2014; Dragovic et al., 2011, 2013; Gercel-Taylor et al., 2012; Varga et al., 2014; Yoshioka et al., 2013). Typical size distributions of EVs start at ~30 nm, show a peak at a

* Corresponding author at: Room A327b, Viikinkaari 4, 00014, University of Helsinki, Helsinki, Finland.
E-mail address: sami.valkonen@helsinki.fi (S. Valkonen).

http://dx.doi.org/10.1016/j.ejps.2016.09.008

diameter <100 nm, and follow a decreasing power-law function or exponential function for diameters >100 nm (Fraikin et al., 2011; van der Pol et al., 2016). With the exception of transmission electron microscopy (TEM), none of the current analytical methods are able to detect the entire population of EVs (van der Pol et al., 2016). The inability to detect the smallest EVs leads to both differences and underestimation of the determined concentration. Consequently, the reported number of EVs in normal human plasma ranges from 10^4 to 10^{12} mL^{-1} (van der Pol et al., 2014a). This 8 orders of magnitude difference in EV concentrations emphasizes the need for standardization.

In flow cytometry, which is one of the most commonly used methods in EV studies (Lacroix et al., 2010), particle detection is often based on light scattering. Because the RI of silica (1.45) and polystyrene beads (1.61) is higher than the mean RI of naturally occurring EVs (~1.39), applying a gate on the scatter signals of silica or polystyrene beads will result in erroneous estimations of EV size and concentration (van der Pol et al., 2012, 2014b). For example, a lower size gate set with 200 nm polystyrene beads, which scatter the same amount of light as EVs of ~500 nm (Chandler et al., 2011), leads to the exclusion of EVs between 200 and 500 nm (van der Pol et al., 2014b). Since the concentration of EVs decreases with increasing diameter, a polystyrene size gate generally leads to an underestimation of the actual EV concentration.

With nanoparticle tracking analysis (NTA) the Stokes–Einstein equation is used to derive the hydrodynamic diameter of EVs from their Brownian motion (Dragovic et al., 2011). Although in NTA, the RI of EVs does not affect the measured diameter, the EV size distribution and RI do affect the measured concentration (Filipe et al., 2010), because the measured concentration depends on the brightness of the scattering particle.

Altogether, these examples emphasize the urgent need to develop RM with a similar RI and size distribution, but preferably also with a morphology (for TEM) and zeta potential (for tunable resistive pulse sensing, TRPS) similar to the studied EVs. Ultimately, also other RM properties would match those of EVs, including surface molecules or internal cargo. This is challenging because the development of an optimal RM for EV studies and the analytical methods for their detection are dependent on each other. Further, the different analytical techniques depend on different properties of EVs (Table 1). In this study, we took a three-step approach to develop RM for EV studies: a literature search was performed to find candidates for biological RM, and then EV researchers were asked for the preferences for RM and their use. Finally, we took a step forward and developed an erythrocyte-derived EV-RM, nanoerythrosomes (NanoE), and evaluated its usability.

2. Materials and Methods

2.1. Literature Search

The task of discovering a potential biological RM for EV studies was initiated through discussions with various professionals of "Metrological characterization of micro-vesicles from body fluids" (METVES; www.metves.eu) program. Based on the discussions, the initial categories of RM were determined and a literature search was conducted in Google and PubMed using terms such as "erythrocyte ghost", "RBC carrier", "outer membrane vesicles", "nanobacteria", "viral particle", "coccoid bacteria", "liposome", "cell organelle", "stability", production", and "preparation" to elaborate the properties of potential RM. Initial inclusion criteria for potential RM were submicron size and organic composition. To further investigate the benefits of the selected RM, experts from the EV field were consulted regarding the properties of potential RM from the literature search. Candidates were excluded if the particles contained infection risk, did not express sufficient physical and biochemical resemblance to EVs, or were poorly storable. The literature search and expert consultation was conducted from 10/2014 to 11/2014.

Table 1
Dependency of the different detection techniques on EV properties and EV sample properties.

	AFM	DLS	FCM	NTA	SAXS	TEM	TRPS
Adhesion	+	−	−	−	−	+	−
Buoyancy	−	−	−	−	−	−	±
Charge	−	±	−	±	−	−	+
Concentration	+	+	+	+	++	+	+
Membrane proteins	±	−	±	±	−	±	−
Monodispersity	−	++	−	±	++	−	−
Refractive index	−	+	++	+	−	−	−
Size	−	+	+	+	++	−	+
Spherical shape	−	++	++	+	+	−	++
Stiffness	+	−	−	−	−	+	−

Abbreviations: AFM: atomic force microscopy; DLS: dynamic light scattering without charge option; FCM: flow cytometry; NTA: nanoparticle tracking analysis without charge option; SAXS: small-angle X-ray scattering; TEM: transmission electron microscopy; TRPS: tunable resistive pulse sensing.

2.2. Survey of RM and Their Use in EV Studies

A questionnaire (Appendix 1) was designed to collect the following information: methods in use for the characterization and quantification of EVs, current use of RM, desired and minimal physical and biochemical requirements of RM, and opinions of other potential RM. The questionnaire was sent to 14 stakeholders from the METVES program and 32 collaborators from the Laboratory of Experimental Clinical Chemistry (Academic Medical Center, Amsterdam, Netherlands) working with EVs. Replies were collected from 11/2014 to 12/2014.

2.3. Preparation of RM from Erythrocyte Concentrates

Standard leukocyte-reduced erythrocyte concentrates were used to produce NanoE. Outdated concentrates were obtained from Sanquin (Amsterdam, The Netherlands) and the Finnish Red Cross Blood Service (Helsinki, Finland). Concentrates were handled anonymously, and only concentrates that could not be administered clinically were used as accepted by the Finnish Supervisory Authority for Welfare and Health (Valvira, Finland).

To isolate erythrocyte-derived EVs (eryEVs), 25 mL of the concentrate was diluted with 25 mL of 0.22 μm filtered calcium- and magnesium-free 1× phosphate-buffered saline (PBS [Sigma-Aldrich, St. Louis, MO, USA]) and centrifuged for 20 min at 1560×*g*, room temperature (RT) without brake (Centrifuge 5810 R, Eppendorf, Hamburg, Germany) (Varga et al., 2014). Supernatant was transferred to new tubes and centrifuged 3 times under the same settings. The obtained supernatant was centrifuged for 1 h in 100,000×*g* at 4 °C (Optima™ MAX-XP Ultracentrifuge with rotor TLA-55, k-factor 66, Beckman Coulter, Brea, CA, USA), after which the pellet was washed with similar ultracentrifugation. Finally, the pellet was suspended with PBS to the initial volume and aliquoted to 100-μL aliquots for storage at −70 °C (Fig. 1A).

NanoE production was initiated by separating the erythrocytes from the concentrate: 25 mL of concentrate was diluted with 25 mL cold (+4 °C) PBS and centrifuged at 300×*g* for 10 min at 4 °C without a brake (Centrifuge 5810 R). The pellet was suspended to an equal volume of cold PBS, centrifuged 1560×*g* for 20 min at 4 °C without a brake (Centrifuge 5810 R). The washing was repeated 2 more times. Next, three different disruption methods were evaluated to produce NanoE:

Freeze-thawing: 500 μL aliquots of erythrocytes were treated with 3 consecutive freeze–thaw cycles of 5 min in liquid nitrogen and 5 min in 37 °C water bath.

N_2 bomb treatment: 5 mL of erythrocytes were diluted with 10 mL of PBS in 50 mL Falcon tube to facilitate nitrogen access to the cells. The tubes were placed in N_2 bomb (Parr Cell Disruption Bomb, Moline, IL, USA). A pressure of 75 Psi was created using nitrogen and after

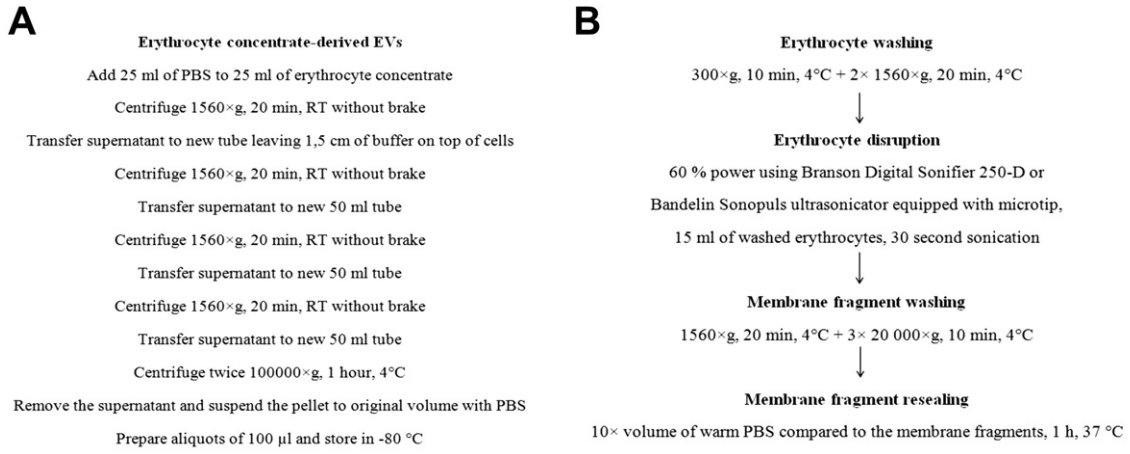

Fig. 1. A step-by-step protocol for harvesting EVs from erythrocyte concentrate (A) and schematic of the production of nanoerythrosomes (B).

30 min, the pressure was gently released and the sample was collected in a 50 mL Falcon tube.

Ultrasonication: 15 mL of erythrocytes were sonicated in an ice bath with either Branson digital sonicator 250-D (Branson Ultrasonics, Danbury, CT, USA) equipped with microtip using continuous sonication, 60% power and 30 or 45 s sonication, or Bandelin Sonopuls ultrasonicator (BANDELIN electronic GmbH & Co. KG, Berlin, Germany) equipped with MS73 microtip and 30 s continuous ultrasonication.

After disruption, the suspensions containing membrane fragments were diluted with an equal volume of cold PBS, and centrifuged for 1560×*g* at 20 min and +4 °C without brake (Centrifuge 5810 R) to remove remaining cells and larger fragments. Remnants were washed by transferring 500 µL aliquots of supernatant to Eppendorf tubes, diluting the suspension 1:1 with cold PBS and centrifuging 10 min in 20,000×*g* for 10 min and +4 °C without brake (Mikro 200R, Andreas Hettich GmbH & Co. KG, Tuttlingen, Germany). Remnants were washed 3 times by suspending the pellet in 1 mL of cold PBS. The washed pellet was suspended in 100 µL of +37 °C PBS and transferred into 10× volume of +37 °C PBS to allow the resealing process at +37 °C (water bath) for 1 h. After the resealing process, the NanoE were aliquoted to 100 µL aliquots and stored in −70 °C.

2.4. Transmission Electron Microscopy

Samples were fixed 30 min in 0.1% (weight/volume, *w*/*v*) paraformaldehyde (Electron Microscopy Sciences, Hatfield, PA). Next, a 200-mesh EM copper grid with formvar coating (Electron Microscopy Sciences) was placed on top of a sample (10 µL), and incubated for 7 min at RT. The grids were transferred to 1.75% uranyl acetate (*w*/*v*) for negative staining. The grid was imaged using a Tecnai 12 transmission electron microscopy (TEM, FEI Company, Eindhoven, The Netherlands), operated at 80 kV.

2.5. Nanoparticle Tracking Analysis

The same NanoE samples were measured with the instruments LM14C, NS300, and NS500 using the same settings (camera level 8, 3 videos of 90 s, 10,000-fold dilution). Analysis of the acquired videos was performed with threshold 5 and gain 10. The used NTA instruments and their specifications are listed in Table 2. LM14C was also used to study how storage affects the size distribution and the concentration of NanoE. NanoE samples were first measured with NTA immediately after preparation and then up to 10 weeks with biweekly measurements (Supplementary Fig. 1).

2.6. Flow Cytometry

NanoE and eryEVs were characterized using Apogee A50 micro (Apogee Flow Systems, Hertfordshire, UK) equipped with a 405 nm laser for measuring scatter and a 488 nm laser for measuring fluorescence. Fluorescence light was spectrally filtered by bandpass filters (525/50, 575/30), and a long pass filter (650 nm). Particles were labeled with a FITC-labeled anti-CD235a antibody (clone 11EB-7-6, Beckman Coulter, Brea, CA, USA) and a lipid dye Di-8-ANEPPS (Invitrogen, Waltham, MA, USA). For CD235a, the NanoE and eryEVs concentration was ~10^8 mL^{-1} as determined by NTA (LM14C). The labeling volume was 100 µL. Possible antibody aggregates were removed before use by centrifuging for 5 min at 18,890×*g* and 20 °C without brakes, and 10 µL of the antibody was used for each sample. After 30 min incubation in the dark, the labeling reaction was stopped by adding 900 µL of 0.22 µm filtered PBS. IgG1-FITC was used as an isotype control (clone MOPC-21, BD Pharmingen, San Jose, CA, USA). For the Di-8-ANEPPS labeling, 1 µL of 12.5× Di-8-ANEPPS lipid dye preparation (1 µL Di-8-ANEPPS, 6.25 µL pluronic acid (product code #P3000MP [Thermo Fisher, Waltham, MA, USA)], and 5.25 µL mQ water) was added to 200 µL samples of eryEVs and NanoE at a concentration of ~10^7 mL^{-1}. As free Di-8-ANEPPS aggregates in the buffer, the amount of Di-8-ANEPPS-positive particles in the buffer without EVs was deducted from samples in data analysis. Samples were incubated for at least 30 min, RT, covered from light. For sample detection, large-angle light scattering or small-angle light scattering was used as a trigger and used voltages and thresholds were 320 and 31 for large-angle light scattering and 295 and 14 for small-angle light scattering, respectively. Samples were injected at 4.5 µL/min, data was collected for 120 s for each sample and three washing cycles were performed between the samples. NanoE and eryEVs were additionally compared to bead mixture of silica and polystyrene beads (Apogee Flow Systems).

2.7. SDS-PAGE

The protein compositions of eryEV and NanoE samples were studied by loading equal amounts of 0.3 µg of protein (determined with µBCA kit [Thermo Fisher Scientific]) together with Multicolor broad range protein ladder (Thermo Fisher Scientific) to commercial Mini-Protean TGX 10% gels (BioRad, Hercules, CA, USA). The gels were run with 180 V for 1 h in 1× Tris/glycine/SDS buffer (BioRad). The gel was fixated (30% ethanol, 0.5% acetic acid [Merck, Kenilworth, NJ, USA]) for 1 h, after which it was rinsed for 10 min in 20% ethanol and 10 min in water. The gel was sensitized using freshly prepared sodium thiosulphate (0.02 g/100 mL [Sigma-Aldrich]) for 1 min. The gel was rinsed twice in water for 20 s and stained in freshly prepared silver nitrate (0.1 g/50 mL

Table 2
Specifications of the NTA instruments and software.

NTA instrument	Laser	Camera	Software version in data collection	Software version in data analysis
LM14C	Violet laser: 405 nm, 70 mW (Malvern Instruments Ltd., Malvern, UK)	sCMOS camera (Hamamatsu Photonics K.K., Hamamatsu, Japan)	3.0	3.1
NS300	Violet laser: 405 nm, 65 mW (Malvern Instruments Ltd.)	sCMOS camera (Hamamatsu Photonics K.K.)	3.1	3.1
NS500	Violet laser: 405 nm, 45 mW (Malvern Instruments Ltd.)	EMCCD camera (Andor Technology, Tokyo, Japan)	3.1	3.1

[Merck]) for 30 min. The gel was rinsed in water for 10 s, after which it was developed using freshly prepared development solution (70 μL of 37% formaldehyde [Merck], 3 g of potassium carbonate [Sigma-Aldrich], 1 mg of sodium thiosulphate [Sigma-Aldrich], and added to 100 mL of water) for 4 min. The development was stopped with incubation in stopping solution (50 g/L Tris base [Merck], 2.5% acetic acid [Merck]) for 1 min, after which the gel was stored in water. The Western blots were prepared as mentioned before (Aatonen et al., 2014).

2.8. Determination of Refractive Index

The RI of NanoE and eryEVs were determined by independently measuring the diameter and the light scattering power of individual particles with NTA and solving the inverse scattering problem with Mie theory (van der Pol et al., 2014b).

2.9. Statistics

Statistical significance was determined by using two-tailed *t*-test (GraphPad Prism v.5.0.1.)

3. Results

3.1. Literature Search

Although several studies have characterized and described the use of monodisperse (Lacroix et al., 2010; Chandler et al., 2011; Maas et al., 2015) and bimodal (Nicolet et al., 2016) synthetic RM, the reported use of biological RM is limited (van der Pol et al., 2012; Anon., n.d.-a). The following literature search describes potential, naturally occurring or "produced" RM, which could be further developed for EV analyses.

3.1.1. Naturally Occurring Sources for Biological RM

Submicron particles with physical and biochemical properties similar to EVs can be isolated from naturally occurring sources. These may include 1) isolated EV populations from, e.g. cell cultures, 2) plasma lipoproteins, plant and marine viruses, and 3) small spherically shaped (coccoid) bacteria, or picoplankton (Table 3).

(1) Potential EV sources are *in vitro* cell cultures (Lazaro-Ibanez et al., 2014), cultures of *Dictyostelium discoideum* (Tatischeff et al., 2012), therapeutic clinical grade erythrocyte (Varga et al., 2014) and platelet (Black et al., 2015) concentrates, urine (van der Pol et al., 2014a), and outer membrane vesicles produced by bacteria (Biller et al., 2014). Here, the specific advantage is that the obtained RM have enhanced physical and biochemical similarities, including the molecular contents, with actual EVs. These EV sources are also fairly accessible and safe. Thus, well-characterized EVs would also be the perfect EV-RM candidates.

(2) Lipoproteins and viral particles from plant and marine sources are suitable as EV-RM because they have a size distribution overlapping with the bulk of EVs (Aatonen et al., 2014; Arraud et al., 2014; Dragovic et al., 2011; Dragovic et al., 2013; Gercel-Taylor et al., 2012; Varga et al., 2014; Yoshioka et al., 2013; Anon., n.d.-b, n.d.-c; Oster, 1950; van Antwerpen et al., 1999; Sawle et al., 2002; McFarlane et al., 2005) and they do have a relatively small variation in size (van Antwerpen et al., 1999; Sawle et al., 2002; McFarlane et al., 2005; Salpeter and Zilversmit, 1968; Colhoun et al., 2002). However, a major drawback of lipoproteins and viral particles is that the RI of these particles is higher than the RI of EVs, due to their high protein content, a prominent problem especially of protein-enveloped viruses. Another issue of using viral particles is their biosafety, which could be circumvented by producing virus-like particles, i.e. particles lacking the viral genome. The mass production of virus-like particles is possible in plant or insect cells (Machida and Imataka, 2015; Santi et al., 2006).

(3) Another possible source of biological RM are non-pathogenic bacteria and picophytoplankton, i.e. aquatic organisms of both prokaryotic and eukaryotic origin ranging between 600 nm and 2000 nm in diameter (Anon., n.d.-d). Several non-pathogenic marine bacteria and picophytoplankton strains exist (personal communication with representatives of Roscoff Culture Collection; Roscoff, France) and can be purchased for culturing. The benefit of cultures of non-pathogenic bacteria and picophytoplankton is that the cultures could be harnessed into mass production to provide two populations of particles with different size distributions. Bacteria can be used as larger particles (>600 nm) and the corresponding bacteria-derived outer membrane vesicles can be used as smaller particles (<250 nm) (Biller et al., 2014). As outer membrane vesicles have comparable physical and biochemical properties as the bacteria (Biller et al., 2014), the main difference would be their size. By maintaining cultures, the biological RM would be essentially self-generating with affordable and effortless maintenance depending of the used strain. A literature search for non-pathogenic bacteria species, which could be used as biological RM based on their size, suggested several spherically shaped (coccoid) bacteria with reported diameters of <1000 nm (Bae et al., 1972; Balkwill and Casida, 1973; Barbier et al., 1999; Lai et al., 2000; Osburn and Amend, 2011).

3.1.2. Production of Biological RM

Besides harvesting EVs as RM from naturally occurring sources, submicron particles with EV-like properties can be produced from various sources. Here, we included particles produced only from biological materials including disrupted cells and different lipid constructs (Table 4).

Biological RM can be produced by disrupting cells to produce small vesicles from the fragments yielding particles with varying diameters (Marchesi and Palade, 1967; Heidrich and Leutner, 1974; Lin and Macey, 1978; Yoon et al., 2015; Jo et al., 2014). The main advantage of using such materials is that the physical and biochemical properties of the obtained RM would better resemble EVs compared to synthetic RM (Yoon et al., 2015; Jo et al., 2014). Erythrocytes are theoretically

Table 3
Naturally occurring potential biological reference materials (RM).

RM	Diameter (nm)	Polydispersity (CV)	RI	Resemblance to EVs	Considerations	References
EVs from						
Cell lines	30–1000	>20%	~1.38	5	EVs stable for months when stored −80 °C	Lazaro-Ibanez et al. (2014)
Dictyostelium discoideum	50–300	35%–70%	–	5	–	Tatischeff et al. (2012)
Erythrocyte or platelet concentrates	10–350	>20%	–	4/5	EVs stable for months when stored −80 °C	Varga et al. (2014), Black et al. (2015)
Lyophilized exosomes*	30–100	>20%	1.37–1.39	5	Commercially available, can be stored for months	Anon. (n.d.-e)
Outer membrane vesicles from (marine) bacteria	10–350	–	–	5	–	Biller et al. (2014), Li et al. (1998), Kadurugamuwa and Beveridge (1997), Schooling and Beveridge (2006), Beveridge (1999)
Urine	45–500	35%–40%	1.37	5	EVs stable for months when stored −80 °C	van der Pol et al. (2014a, 2014b), Tatischeff et al. (2012)
Lipoproteins						
High-density lipoproteins	6–15	~5%	1.45−1.6	4	Must be stored under nitrogen or argon, if stored in +4 °C. Can be stored at −80 °C for months	van der Pol et al. (2014b), van Antwerpen et al. (1999), Sawle et al. (2002), McFarlane et al. (2005), Salpeter and Zilversmit (1968), Colhoun et al. (2002), Perusse et al. (2001), Wood et al. (2006)
Low-density lipoproteins	18–25	<10%				
Intermediate-density lipoproteins	30	~1.5%				
Very low-density lipoproteins	30–80	~20%				
Chylomicrons	200–600	>20%				
Viral particles from						
Marine virus species	110–130	<20%	–	2	Can be stored for months in −80 °C. No safety restrictions, if particles do not contain genomic material	Anon. (n.d.-d)
Plant virus species	20–85	<20%	1.52–1.57	2		van der Pol et al. (2014b), Anon. (n.d.-b, n.d.-c) Oster (1950)
Coccoid-shaped organisms						
Aquatic bacteria/pico(phyto)plankton	300-1000	–	1.35-1.47**	5	Can be stored for months in −80 °C. No safety restrictions, if particles do not contain genomic material.	Biller et al. (2014), Anon. (n.d.-d), Lai et al. (2000), Ackleson and Spinrad (1988), Spinrad and Brown (1986), Kuo et al. (2014), Hashemi et al. (2011)
Nanobacteria from soil	200–1000	–	–	5		Bae et al. (1972), Balkwill and Casida (1973)

RM were categorized according to size, polydispersity, refractive index (RI), and the resemblance to the EVs. Resemblance to EVs was scored on 1–5 points depending on whether the RM has (1) no resemblance, (2) proteins and genomic material but no lipid membrane, (3) phospholipid membrane, (4) phospholipid membrane containing proteins, or (5) phospholipid membrane containing proteins and genomic material. * = Exosomes from HansaBiomed, Tallinn, Estonia. ** = Values based on the references and the refractive index of water at 488 nm.

ideal materials to use, since their cell membrane composition is well-characterized and they are devoid of intracellular membranes (Virtanen et al., 1998). Additionally, erythrocytes are structurally stable during extended storage (Chaplin, 1982) and are an easily accessible material. For these reasons, erythrocytes from clinical surplus concentrates were used to produce an RM for testing and evaluation. Different

Table 4
Produced biological reference materials (RM). RM were categorized according to size, polydispersity, refractive index (RI), and the resemblance to the EVs.

RM	Diameter (nm)	Polydispersity (CV)	RI	Resemblance to EVs	Considerations	References
Disrupted cells						
Preparation method A	<200	>20%	–	4	–	Marchesi and Palade (1967)
Preparation method B	200–700	>20%	–	4	–	Heidrich and Leutner (1974)
Preparation method C	100–5000	>20%	–	4	–	Lin and Macey (1978)
Preparation method D	100–300	20%–35%	–	5	–	Yoon et al. (2015)
Preparation method E	100	–	–	5	–	Jo et al. (2014)
Lipid constructs						
Liposomes	100	~5%	1.363–1.392	3	–	Lapinski et al. (2007), Matsuzaki et al. (2000)
Liposomes (commercially available*)	100 and 500	<20% for smaller particles, >20% for bigger particles	Varies with used buffer	3-5	Can be stored at least 12 months	Anon., (n.d.-f)
Lipoparticles**	191	13%	–	3-4	Can be stored for 18 months	Anon. (n.d.-g)
Oil droplets***	<100	<20%	Engineered to preferred RI	1	Can be stored at least 12 months	Anon. (n.d.-h, n.d.-i),

Resemblance to EVs was scored from 1 to 5 points depending on whether the RM has (1) no resemblance, (2) proteins and genomic material but no lipid membrane, (3) phospholipid membrane, (4) phospholipid membrane containing proteins, or (5) phospholipid membrane containing proteins and genomic material. * = Liposomes from Excytex, Zeist, The Netherlands; ** = lipoparticles from Integral Molecular, Philadelphia, PA, USA; *** = oil from Apogee Flow Systems, Hertfordshire, UK or Cargille Laboratories, Cedar Grove, NJ, USA.

methods for erythrocyte disruption were compared, and a method for NanoE production was developed (Fig. 1B). An additional advantage of using erythrocytes is that they can be used to produce two types of biological RM for comparison: 1) by disrupting the erythrocytes NanoE are formed, and 2) by harvesting the spontaneously shed eryEVs.

Biological RM can also be obtained from lipid constructs such as liposomes that are extensively used as delivery vehicles (Allen and Cullis, 2004; van der Meel et al., 2014) and their production methods are well known. Liposomes of a desired size can be prepared by ultrasonication or extrusion of the starting material through polycarbonate filters of a set pore size (Lapinski et al., 2007; Akbarzadeh et al., 2013). As the liposomes are produced from bulk material, their composition is well characterized. Especially, liposomes with a small diameter (~70 nm) prepared by extrusion have <20% variation in size (CV, ratio of the standard deviation to the mean, expressed as percentage) (Garcia-Diez et al., 2016). An advantage of liposomes is that their RI can be manipulated during the production (Fenzl et al., 2015). Another type of RM resembling liposomes are non-infectious virus-like particles called lipoparticles, which consist of a lipid membrane constructed on top of a protein core. These lipoparticles have a well-defined diameter of ~190 nm with a narrow size distribution (CV = 13%), and they are stable during storage. On request, additional proteins could be attached to the lipoparticle surface, which will increase their biochemical similarity to EVs.

Finally, as a non-biological exception, we include oil droplets as one option of a produced RM because they would offer close similarity with EVs regarding the size and RI. As with liposomes, extrusion can be used to prepare oil droplets of a specific size from oils of commercial providers. The advantage of using oil droplets is that the RI can be designed exactly, thus improving their resemblance to EVs (personal communication with Oliver Kenyon, CEO of Apogee Flow Systems, Hertfordshire, UK and representatives of Cargille Laboratories, Cedar Grove, NJ, USA).

3.2. Survey

The literature search revealed several different types of RM, which had varying benefits and drawbacks. Therefore, the opinions of laboratories working with EVs were surveyed through a questionnaire to discover the requirements of biological RM by the end-users. A questionnaire (Appendix 1) was sent to 46 laboratories and the response rate was 44%. Flow cytometry was indicated as the most common method for EV studies (90% of the responders; Fig. 2A),

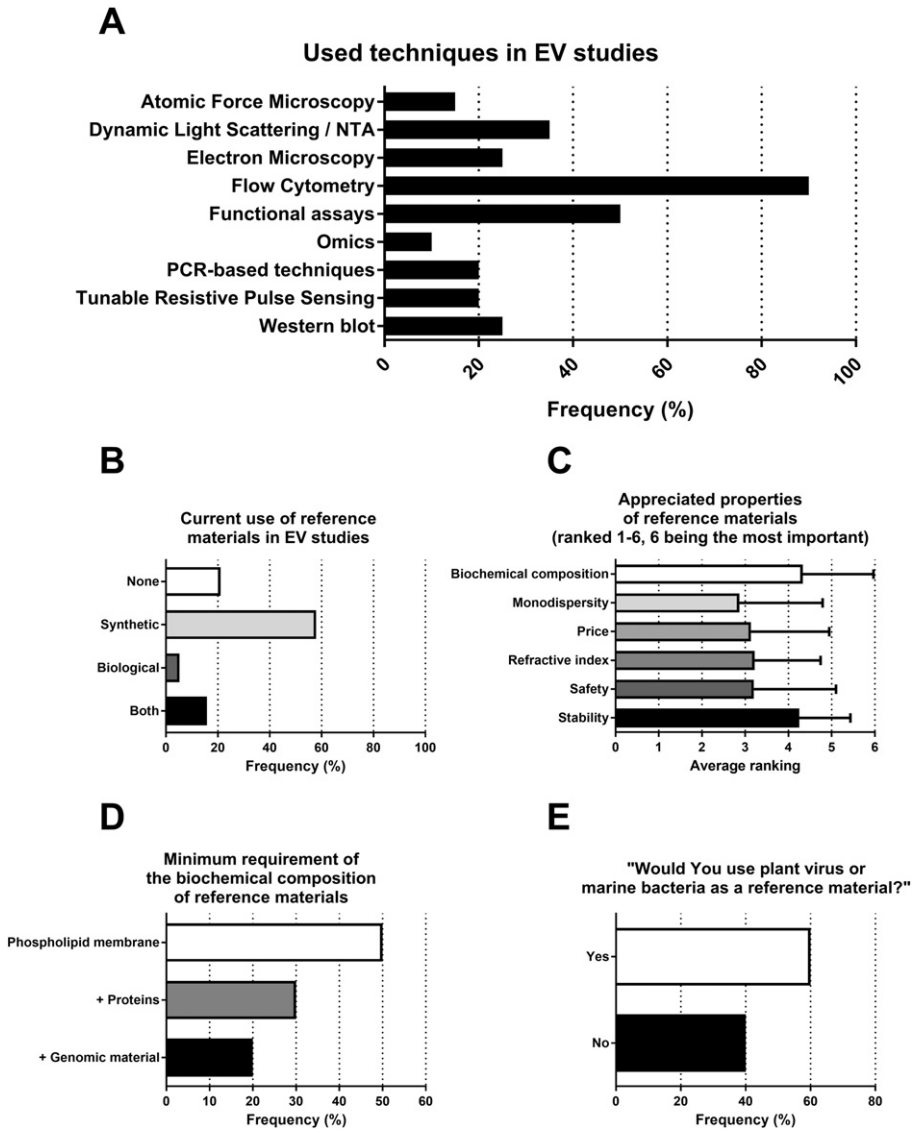

Fig. 2. Results from 46 EV laboratories based on a questionnaire asking (A) which techniques were in use for EV studies (multiple choices allowed); (B) currently used RM; (C) preferred properties for optimal RM; (D) minimal requirements for a RM; and (E) willingness to use plant viruses/marine bacteria as RM. Values represent mean ± S.D. Published previously (in www.metves.eu), reproduced with permission. NTA = nanoparticle tracking analysis; PCR = polymerase chain reaction.

underlining the need for a RM with a size and RI distribution resembling EVs. Besides using functional assays (50%), dynamic light scattering/NTA (35%), electron microscopy (25%), and Western blotting (25%) were listed as the most commonly used techniques for EV studies (Fig. 2A). When laboratories were asked whether they have used an RM in their studies, the majority reported using synthetic RM (58%), 5% used biological RM, and 16% used both. However, 20% used no RM in their EV studies (Fig. 2B).

The laboratories were asked to rank the order of importance regarding the desired properties, i.e. the biochemical composition, monodispersity, price, refractive index, and safety. The biochemical composition (average rank of 4.33/6) and stability (average rank of 4.25/6) were indicated as the most important properties (Fig. 2C). Next, price, RI, and safety were listed with an almost equal importance (average ranks of 3.13/6, 3.21/6, and 3.20/6, respectively), whilst monodispersity was considered as the least important property (average rank of 2.90/6) (Fig. 2C). Regarding the requirements for the structural properties, 50% of the laboratories working with EVs would be satisfied if the RM would contain a phospholipid membrane, 30% would additionally require proteins, and 20% would require a phospholipid membrane and the presence of both proteins and genomic material (Fig. 2D). Finally, 60% would be willing to use plant viruses and marine bacteria as RM, provided that their biosafety can be assured (Fig. 2E).

3.3. NanoE Production

NanoE were selected as a biological RM candidate, based on the literature review and the survey responses. Three erythrocyte disruption methods (freeze–thaw cycles, N_2 bomb, and ultrasonication) were tested in the NanoE production. Freeze–thaw cycles did not break down the erythrocytes sufficiently, as seen in TEM micrographs (Fig. 3A), although the treatment made the erythrocytes leaky, resulting in white erythrocyte ghosts. Furthermore, the number of submicron particles was almost non-existent (Fig. 3B). Disruption using an N_2 bomb resulted in either intact or completely shattered erythrocytes (Fig. 3C), and similar to the freeze–thaw treatment, submicron particles were almost non-existent (Fig. 3D). Finally, ultrasonication disrupted erythrocytes almost completely (Fig. 3E), producing a concentration of submicron particles higher than the application of freeze–thaw cycles or an N_2 bomb (Fig. 3F). Despite using different ultrasonicators, the size distribution profile of the produced NanoE was similar (data not shown). Extending the length of the ultrasonication treatment from 30 s to 45 s decreased the final particle concentration without affecting the size distribution (Fig. 3G and H). Based on the results, an additional washing step was included in the final protocol to remove any remaining intact cells and larger cell fragments, seen especially in freeze–thaw cycle and N_2 bomb disruptions.

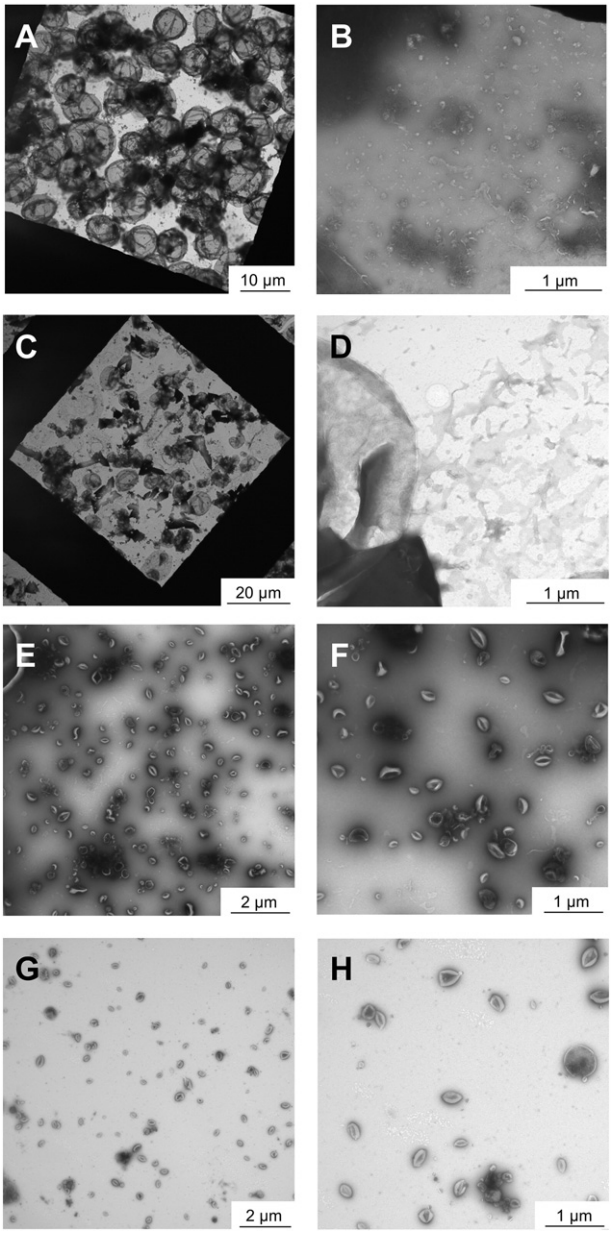

Fig. 3. Representative transmission electron microscope micrographs of erythrocytes disrupted by three consecutive freeze–thaw cycles (A and B), by an N_2 bomb (C and D), by a 30-s ultrasonication (E and F), and by a 45-s ultrasonication (G and H).

3.4. EryEVs vs. NanoE

To examine the usability of NanoE as RM, their physical and biochemical properties were compared with the naturally occurring eryEVs from the same concentrate. The morphology of eryEVs and NanoE was similar as inspected by TEM (Fig. 4A and B). Also, the RI distribution and mean RI (1.37) measured by NTA were similar for eryEVs and NanoE (Fig. 4C). The protein content of NanoE was considerably different from eryEVs as shown by SDS-PAGE (Fig. 4D). Enriched proteins in Western blotting of NanoE vs. eryEVs were, e.g. hemoglobin and Band 3 (data not shown). The size of NanoE was slightly greater than that of eryEVs: 66% of the NanoE population was larger than 200 nm, and the main population (58%) was between 200 and 400 nm, whereas only <30% of eryEVs were larger than 200 nm when determined by NTA (Fig. 4E). The difference in size distribution was also observed in flow cytometry, where a majority of NanoE were found in the same area as 180 nm silica beads in contrast to the smaller eryEVs (Fig. 4F).

Next, flow cytometry was used to determine the fraction of Di-8-ANEPPS positivity and CD235a antigen density of eryEVs and NanoE. Lipid labeling of NanoE by Di-8-ANEPPS showed a higher percentage of labeled particles compared to the eryEVs (67% vs. 45% respectively, $p < 0.05$, Fig. 5). Similarly, the CD235a labeling was significantly higher for NanoE than for eryEVs (58% vs. 21%, respectively, $p < 0.0001$, Fig. 6, fluorescence intensity 68.3 ± 21.6 vs. 40.5 ± 13.0).

3.5. Application of NanoE as a Biological RM to Standardize EV Measurements

To demonstrate the relevance of using a biological RM for the standardization of EV measurements, NanoE was analyzed using three different NTA instruments. The same batch of NanoE was measured using the same settings optimized for the LM14C instrument, which were then applied during measurements with NTA models NS300 and NS500. The size distribution of the detected particles was similar

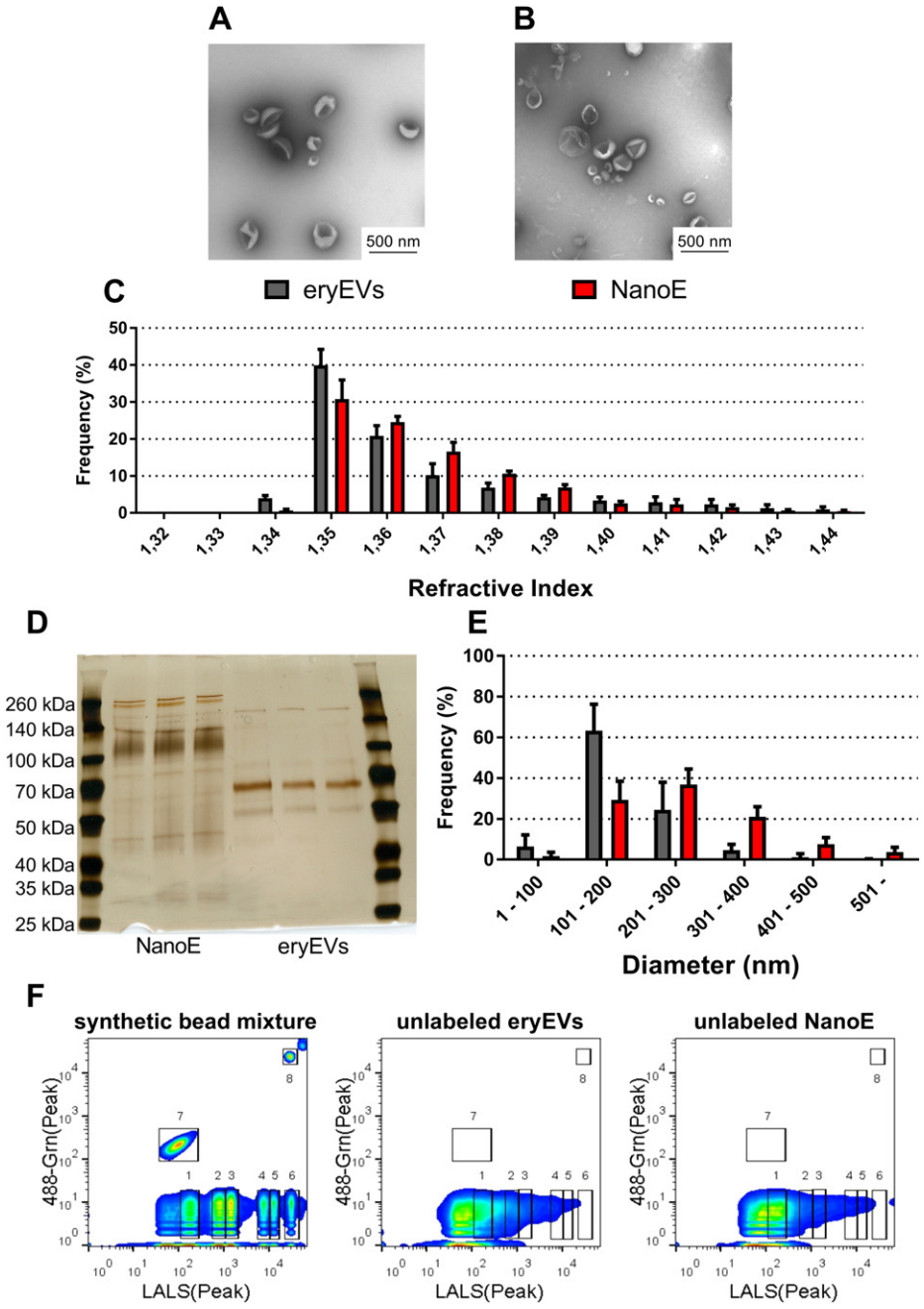

Fig. 4. Comparison of erythrocyte-derived EV (eryEVs) and nanoerythrosomes (NanoE) showing transmission electron microscopy micrographs from (A) eryEVs and (B) NanoE; (C) refractive index measurements; (D) silver-stained SDS-PAGE gel of NanoE and eryEV samples; (E) size distribution measured by nanoparticle tracking analysis; and (F) polystyrene and silica bead mixture, unlabeled eryEVs, and unlabeled NanoE as detected with flow cytometer. Gate 1 = 180 nm silica beads; gate 2 = 240 nm silica beads; gate 3 = 300 nm silica beads; gate 4 = 590 nm silica beads; gate 5 = 800 nm silica beads; gate 6 = 1300 nm silica beads; gate 7 = (fluorescent) 110 nm polystyrene beads; gate 8 = (fluorescent) 500 nm polystyrene beads. Values represent mean ± S.D., $n = 3$ (C) or 18–20 (E).

among the used NTA instruments, with the majority of particles (~60%) ranging from 200 to 400 nm in diameter (Fig. 7A). However, although the same NanoE concentrations were expected to be measured, the obtained NanoE concentrations varied ~40-fold among the different instruments (Fig. 7B).

4. Discussion and Conclusions

The development of RM for EVs is tightly intertwined with the development of the EV analysis methods as both feed each other's advancement. Although progress has been made with different sizes of monodisperse nanoparticles (van der Pol et al., 2014b; Wang et al., 2008), the analyses of complex mixtures of polydisperse particles are challenging (van der Pol et al., 2016). The European Metrology Research Program has initiated important standardization work in anticipation of the rapid momentum of the EV research field and therefore funded METVES, a program focused on metrological characterization of EVs from body fluids. In collaboration with METVES, this study was performed by a national EV research platform funded as an initiative of a Finnish industry- and university-driven research program SalWe-GID, through which multiple end-users are interested in the EV standardization for their improved utilization. The progress in METVES on synthetic RM and the applicable methods for their analysis encouraged us to try to foresee the further needs for biological EV-resembling RM. In order to

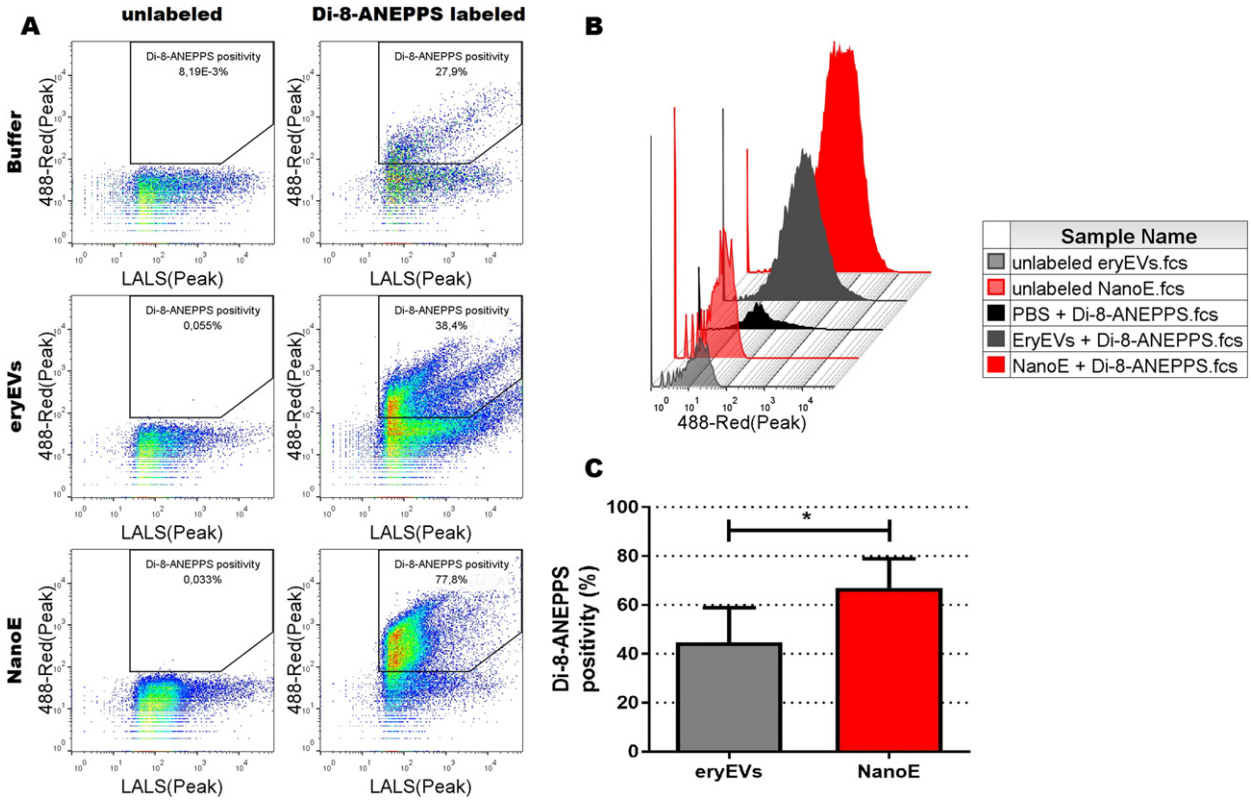

Fig. 5. (A) Apogee A50 dot plots showing the Di-8-ANEPPS labeling of erythrocyte-derived EVs (eryEVs) and nanoerythrosomes (NanoE) compared to negative controls; (B) datagram showing the Di-8-ANEPPS labeling of eryEVs and NanoE compared to negative control; and (C) comparison of Di-8-ANEPPS labeling of eryEVs and NanoE. Values represent mean ± S.D., $n = 6$, * = $p < 0.05$.

gain information on these, a survey was launched. Based on the survey, flow cytometry and synthetic RM were indicated as the most used combination in EV studies, which underpins the problems of RM development. Especially with the flow cytometers, the use of synthetic RM leads to the selection of particles within the size range of cells (van der Pol et al., 2012; Chandler et al., 2011), thereby affecting the conclusions of EV studies particularly from clinical samples such as plasma. Biochemical resemblance to EVs and stability were the most crucial properties for a biological RM according to the laboratories who participated in the survey. As more unusual sources, e.g. plant viruses or marine bacteria, were also acceptable as RM, a wide range of possibilities worth investigating were listed from the literature, if they matched the basic criteria set for RM.

Based on previous results (Anon., n.d.-a), the survey, and the literature review, NanoE was chosen for further development and evaluation as a candidate for biological RM. The optimized method of NanoE production required ultrasonication to disrupt erythrocytes, a method previously used to produce submicron particles from lipids (Lapinski et al., 2007). Upon resealing, the produced particles resembled eryEVs regarding their morphology and RI. The larger size and the enhanced CD235a/Di-8-ANEPPS labeling of NanoE vs. that of eryEVs may be beneficial for their use as EV-RM. Thus, NanoE represents a reasonable option to EV-dedicated flow cytometers and possibly also to earlier models of flow cytometers, which are able to detect 300–700 nm single particles with EV-like RI (van der Pol et al., 2012). The enhanced CD235a positivity may be explained by the instantaneous disruption of erythrocytes, where no selection of surface proteins occurs compared to natural EV budding (Dragovic et al., 2013). This was also supported by the differences of the total protein composition of NanoE and EryEVs. A drawback of NanoE may thus be that since they do not expose common EV surface markers such as CD9, CD63, or CD81 (Yoshioka et al., 2013; Andreu and Yanez-Mo, 2014) nor significant amounts of genomic material, they will not be applicable as RM for methods using these properties as the basis of the analysis. However, the lack of typical EV markers and expression of erythrocyte-specific marker CD235a would enable spiking of EV samples with NanoE, which might be useful in the quantification of EVs from different sources. As such, NanoE can already be utilized as an RM for NTA, TRPS, and flow cytometry.

Comparing the properties of NanoE with those indicated by the survey, NanoE have a matching RI and contain phospholipid membrane and proteins; criteria which fulfil the needs of the majority of the participating EV laboratories. Furthermore, NanoE are relatively stable, safe, and cheap to produce in large quantities from surplus clinical grade erythrocyte concentrates. Although the NanoE population cannot be described as monodisperse, out of the desired properties, monodispersity was ranked as the least important. Monodispersity could be substantially improved by additional preparative steps, thereby allowing the isolation of populations with a narrow size range using different filtration (Zinsser and Tang, 1927), chromatographic (Boing et al., 2014), microfluidics (Ashcroft et al., 2012; Lee et al., 2015), or field-flow fractionation (Petersen et al., 2014; Agarwal et al., 2015) methods. Provided that a monodisperse biological RM could be produced in the future, further characterization by methods such as small-angle X-ray scattering could be, at least hypothetically, used to generate “traceable measurements”, i.e. measurements that could ultimately be related to the SI unit (in this case “metre”) through an unbroken chain of comparisons with known uncertainties (Varga et al., 2014). More realistically, the following step in the development of similarly equivalent standards with NanoE would be the mechanical disruption of platelets or cells from immortalized cell cultures to produce biological RM that would better resemble multiple EV properties, including EV surface markers and internal cargo, and could then be utilized by multiple analytical approaches.

To demonstrate the relevance of biological RM for the standardization of EV measurements, we measured the same batch of NanoE using the same settings on different NTA instruments. The size

distribution of the detected particles was similar, but the obtained NanoE concentrations varied ~40-fold among the NTA instruments, which emphasizes the importance of using an EV-RM. The particle concentration measured by NTA is assumed to be proportional to the mean number of scattering particles in the field-of-view of the microscope, which depends on the intensity and wavelength of the illumination, collection angles of the objective, the sensitivity of the camera with the applied settings (Maas et al., 2015; Gardiner et al., 2013), the analysis software, and the brightness of the scattering particles, which in turn depends on the particle size, refractive index, and concentration (due to multiple and dependent scattering). The differences in the particle concentrations obtained with similar NTA instruments are caused by an inappropriate calibration factor between the mean number of scattering particles in the field-of-view and the provided concentration

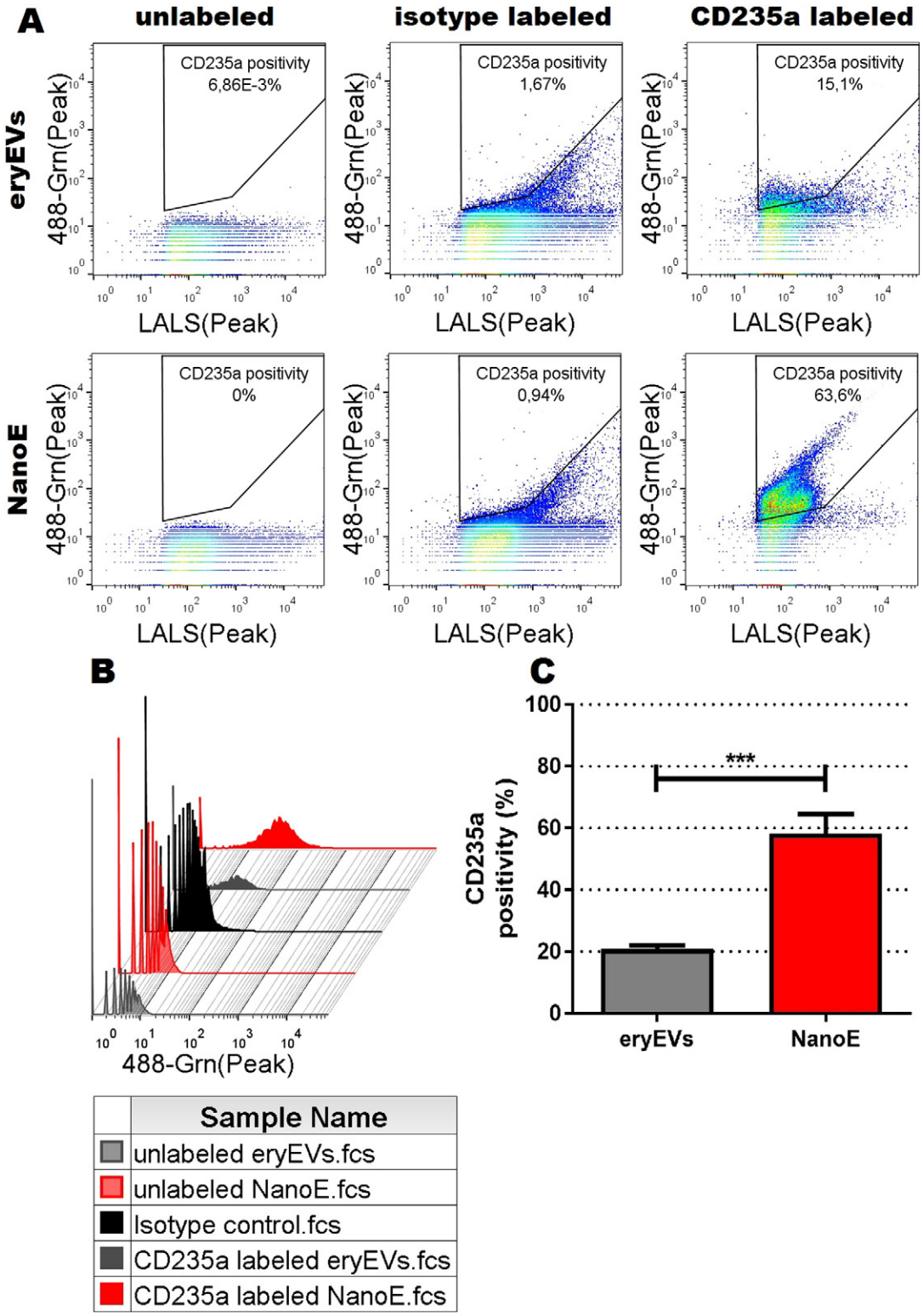

Fig. 6. (A) Apogee A50 dot plots showing CD235a-labeling of erythrocyte-derived EVs (eryEVs) and nanoerythrosomes (NanoE); (B) a datagram showing CD235a-labeling of eryEVs and NanoE; and (C) comparison of CD235a-labeling of eryEVs and NanoE. Values represent mean ± S.D., $n = 6$, *** = $p < 0.0001$.

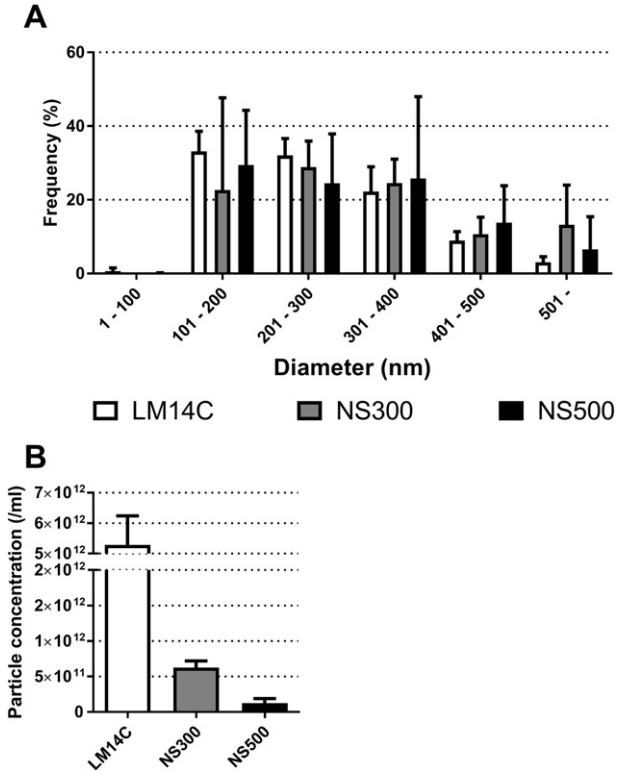

Fig. 7. Characterization of the applicability of the nanoerythrosome standard by measuring the same standard with Nanoparticle Tracking Analysis models LM14C, NS300, and NS500 by (A) particle concentrations and (B) size distribution. Values represent mean ± S.D., $n = 5$.

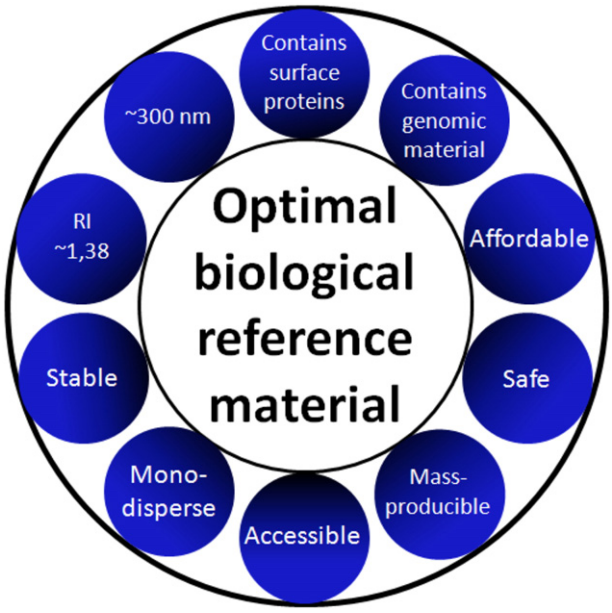

Fig. 8. Optimal properties for a biological reference material for EV studies.

and a lack of knowledge on the diameter of the smallest detectable EVs. Once the concentration of the NanoE can be measured in a traceable way, NanoE can be used to calibrate NTA instruments, i.e. relating the mean number of scattering particles in the field-of-view of NTA to the traceably measured concentration, and defining the smallest detectable EV diameter. In analogy to NTA, other instruments can be calibrated with NanoE to improve the measurement quality within each laboratory. Despite the challenges, EV quantification by particle enumeration is, in most cases, a more accurate way of comparing samples than any indirect EV quantification method such as determination of protein content. The protein content of an EV sample may be independent of the particle number and can vary with the cell activation (Aatonen et al., 2014), the used cell line (Lazaro-Ibanez et al., 2014), and the method by which the protein content is measured (Okutucu et al., 2007). Therefore, direct particle measurements should be favoured in the case of EV quantification and the expressed concentration should be coupled with the knowledge of the detection limits of the instruments/method.

A summary of the optimal properties of a biological RM is presented in Fig. 8, based on the collected information gathered during this study. However, although desirable, it is unlikely that one biological RM would be applicable, not to mention optimal, for all different measurement techniques due to the vast variation in the detection methods (Table 1). Therefore, the search for an optimal biological RM should be approached from a technical perspective, research focus, and considering the EV material. Still, the development of such materials will not be easy.

As the research on EVs progresses, and the use of EVs is pursued in clinical assays and for theranostics, it is crucial to develop various RM to enable precise and reproducible measurements. This will most likely be first achieved by the use of synthetic RM in flow cytometry and in the techniques for EV enumeration. However, the simultaneous development of biological RM would clearly provide additional benefits to the field. Where synthetic RM could be useful for instrument calibration, biological RM could be used for validation of EV measurements. By spreading the RM for common use, the repeatability of studies and the reliability of data will be increased, which in turn will increase the transparency of EV research and improve standardization. Since the discovery of new biological RM for EV studies is a laborious task, it requires the united work of all laboratories and openness. Research networks such as the MEHAD (Extracellular Vesicles in Health and Disease, COST Action BM 1202) and metrological initiatives such as those conducted by METVES, are in a crucial position to take this endeavor to the next level, but ultimately, it is the interest and responsibility of all EV researchers to make this possible.

Abbreviations

eryEVs	erythrocyte-derived extracellular vesicle
EVs	extracellular vesicle
NTA	nanoparticle tracking analysis
NanoE	nanoerythrosome
PBS	phosphate-buffered saline
RI	refractive index
RM	reference material
TEM	transmission electron microscopy
TRPS	tunable resistive pulse sensing

Acknowledgements

Part of this work was funded by SalWe Research Program Personalized Diagnostics and Care (GET IT DONE) (Tekes—the Finnish Funding Agency for Technology and Innovation grant Dnro 3986/31/2013 (SV, MYP, SL, PS).

Part of this work was funded by the European Metrology Research Programme (EMRP) under the Joint Research Project HLT02 (www.metves.eu). The EMRP is jointly funded by the EMRP participating countries within the European Association of National Metrology Institutes and the European Union (SV, YY and RN).

Part of this work was funded by Academy of Finland program grant no. 287089 (PS, SV).

A. Grootemaat and N. Hajji (Laboratory of Experimental Clinical Chemistry, Academic Medical Centre, Amsterdam, The Netherlands) have contributed substantially to the article by performing TEM micrograph processing and data collection.

We would like to thank L. Sankkila (Finnish Red Cross Blood Service, Helsinki, Finland) for the excellent assistance with SDS-PAGE gels.

We acknowledge the kind help of the researchers who participated in the survey.

The authors wish to acknowledge EU H2020 COST Action European Network in Microvesicles and Exosomes in Health and Disease [BM1202].

Appendix A. Supplementary data

Supplementary data to this article can be found online at http://dx.doi.org/10.1016/j.ejps.2016.09.008.

References

Aatonen, M.T., Ohman, T., Nyman, T.A., Laitinen, S., Gronholm, M., Siljander, P.R., Aug 6 2014. Isolation and characterization of platelet-derived extracellular vesicles. J. Extracell Vesicles 3. http://dx.doi.org/10.3402/jev.v3.24692 (eCollection 2014).

Ackleson, S.G., Spinrad, R.W., 1988 Apr 1. Size and refractive index of individual marine participates: a flow cytometric approach. Appl. Opt. 27 (7), 1270–1277.

Agarwal, K., Saji, M., Lazaroff, S.M., Palmer, A.F., Ringel, M.D., Paulaitis, M.E., 2015 May 19. Analysis of exosome release as a cellular response to MAPK pathway inhibition. Langmuir 31 (19), 5440–5448.

Akbarzadeh, A., Rezaei-Sadabady, R., Davaran, S., Joo, S.W., Zarghami, N., Hanifehpour, Y., et al., 2013 Feb 22. Liposome: classification, preparation, and applications. Nanoscale Res. Lett. 8 (1), 102 (-276X-8-102).

Allen, T.M., Cullis, P.R., 2004 Mar 19. Drug delivery systems: entering the mainstream. Science 303 (5665), 1818–1822.

Andreu, Z., Yanez-Mo, M., 2014 Sep 16. Tetraspanins in extracellular vesicle formation and function. Front. Immunol. 5, 442.

Anon., d. Available at: http://www.metves.eu/downloads/reports/METVES_Report_Yuana_2015_Biological_microvesicles%20_reference_materials.pdf (Accessed 4/25, 2016).

Anon., d. Online plant virus databaseAvailable at: http://pvo.bio-mirror.cn (Accessed 10/22, 2014).

Anon., d. Online plant virus databaseAvailable at: http://www.dpvweb.net/index.php (Accessed 10/25, 2014).

Anon., d. Available at: http://roscoff-culture-collection.org (Accessed 10/26, 2014).

Anon., d. Available at: http://www.hansabiomed.eu (Accessed 10/11, 2014).

Anon., d. Available at: http://www.excytex.com (Accessed 4/20, 2016).

Anon., d. Available at: http://www.integralmolecular.com (Accessed 4/20, 2016).

Anon., d. Available at: http://www.cargille.com (Accessed 4/20, 2016).

Anon., d. Available at: http://www.apogeeflow.com (Accessed 4/20, 2016).

Arraud, N., Linares, R., Tan, S., Gounou, C., Pasquet, J.M., Mornet, S., et al., 2014 May. Extracellular vesicles from blood plasma: determination of their morphology, size, phenotype and concentration. J. Thromb. Haemost. 12 (5), 614–627.

Ashcroft, B.A., de Sonneville, J., Yuana, Y., Osanto, S., Bertina, R., Kuil, M.E., et al., 2012 Aug. Determination of the size distribution of blood microparticles directly in plasma using atomic force microscopy and microfluidics. Biomed. Microdevices 14 (4), 641–649.

Bae, H.C., Cota-Robles, E.H., Casida, L.E., 1972 Mar. Microflora of soil as viewed by transmission electron microscopy. Appl. Microbiol. 23 (3), 637–648.

Balkwill, D.L., Casida Jr., L.E., 1973 Jun. Microflora of soil as viewed by freeze-etching. J. Bacteriol. 114 (3), 1319–1327.

Barbier, G., Godfroy, A., Meunier, J.R., Querellou, J., Cambon, M.A., Lesongeur, F., et al., Oct 1999. *Pyrococcus glycovorans* sp. nov., a hyperthermophilic archaeon isolated from the East Pacific Rise. Int. J. Syst. Bacteriol. 49 (Pt 4), 1829–1837.

Beveridge, T.J., 1999 Aug. Structures of gram-negative cell walls and their derived membrane vesicles. J. Bacteriol. 181 (16), 4725–4733.

Biller, S.J., Schubotz, F., Roggensack, S.E., Thompson, A.W., Summons, R.E., Chisholm, S.W., 2014 Jan 10. Bacterial vesicles in marine ecosystems. Science 343 (6167), 183–186.

Black, A., Pienimaeki-Roemer, A., Kenyon, O., Orso, E., Schmitz, G., 2015 Sep. Platelet-derived extracellular vesicles in platelet pheresis concentrates as a quality control approach. Transfusion 55 (9), 2184–2196.

Boing, A.N., van der Pol, E., Grootemaat, A.E., Coumans, F.A., Sturk, A., Nieuwland, R., 2014 Sep 8. Single-step isolation of extracellular vesicles by size-exclusion chromatography. J. Extracell Vesicles 3. http://dx.doi.org/10.3402/jev.v3.23430 (eCollection 2014).

Chandler, W.L., Yeung, W., Tait, J.F., 2011 Jun. A new microparticle size calibration standard for use in measuring smaller microparticles using a new flow cytometer. J. Thromb. Haemost. 9 (6), 1216–1224.

Chaplin Jr., H., 1982 Jun. The proper use of previously frozen red blood cells for transfusion. Blood 59 (6), 1118–1120.

Colhoun, H.M., Otvos, J.D., Rubens, M.B., Taskinen, M.R., Underwood, S.R., Fuller, J.H., 2002 Jun. Lipoprotein subclasses and particle sizes and their relationship with coronary artery calcification in men and women with and without type 1 diabetes. Diabetes 51 (6), 1949–1956.

Dragovic, R.A., Gardiner, C., Brooks, A.S., Tannetta, D.S., Ferguson, D.J., Hole, P., et al., 2011 Dec. Sizing and phenotyping of cellular vesicles using nanoparticle tracking analysis. Nanomedicine 7 (6), 780–788.

Dragovic, R.A., Southcombe, J.H., Tannetta, D.S., Redman, C.W., Sargent, I.L., 2013 Dec 26. Multicolor flow cytometry and nanoparticle tracking analysis of extracellular vesicles in the plasma of normal pregnant and pre-eclamptic women. Biol. Reprod. 89 (6), 151.

Fais, S., O'Driscoll, L., Borras, F.E., Buzas, E., Camussi, G., Cappello, F., et al., 2016 Apr 26. Evidence-based clinical use of nanoscale extracellular vesicles in nanomedicine. ACS Nano 10 (4), 3886–3899.

Fenzl, C., Hirsch, T., Baeumner, A.J., 2015 11/03. Liposomes with high refractive index encapsulants as tunable signal amplification tools in surface plasmon resonance spectroscopy. Anal. Chem. 87 (21), 11157–11163 (2015).

Filipe, V., Hawe, A., Jiskoot, W., 2010 May. Critical evaluation of nanoparticle tracking analysis (NTA) by NanoSight for the measurement of nanoparticles and protein aggregates. Pharm. Res. 27 (5), 796–810.

Fraikin, J.L., Teesalu, T., McKenney, C.M., Ruoslahti, E., Cleland, A.N., 2011 May. A high-throughput label-free nanoparticle analyser. Nat. Nanotechnol. 6 (5), 308–313.

Garcia-Diez, R., Gollwitzer, C., Krumrey, M., Varga, Z., 2016 Jan 26. Size determination of a liposomal drug by small-angle X-ray scattering using continuous contrast variation. Langmuir 32 (3), 772–778.

Gardiner, C., Ferreira, Y.J., Dragovic, R.A., Redman, C.W., Sargent, I.L., 2013 Feb 15. Extracellular vesicle sizing and enumeration by nanoparticle tracking analysis. J. Extracell Vesicles 2. http://dx.doi.org/10.3402/jev.v2i0.19671 (eCollection 2013).

Gercel-Taylor, C., Atay, S., Tullis, R.H., Kesimer, M., Taylor, D.D., 2012 Sep 1. Nanoparticle analysis of circulating cell-derived vesicles in ovarian cancer patients. Anal. Biochem. 428 (1), 44–53.

Hashemi, N., Erickson, J.S., Golden, J.P., Jackson, K.M., Ligler, F.S., 2011 Jul 15. Microflow cytometer for optical analysis of phytoplankton. Biosens. Bioelectron. 26 (11), 4263–4269.

Heidrich, H.G., Leutner, G., 1974 Jan 3. Two types of vesicles from the erythrocyte-ghost membrane differing in surface charge. Separation and characterization by preparative free-flow electrophoresis. Eur. J. Biochem. 41 (1), 37–43.

Jo, W., Kim, J., Yoon, J., Jeong, D., Cho, S., Jeong, H., et al., 2014 Oct 21. Large-scale generation of cell-derived nanovesicles. Nanoscale 6 (20), 12056–12064.

Kadurugamuwa, J.L., Beveridge, T.J., 1997 Nov. Natural release of virulence factors in membrane vesicles by *Pseudomonas aeruginosa* and the effect of aminoglycoside antibiotics on their release. J. Antimicrob. Chemother. 40 (5), 615–621.

Kuo, J., Tew, K.S., Ye, Y.X., Cheng, J.O., Meng, P.J., Glover, D.C., 2014. Picoplankton dynamics and picoeukaryote diversity in a hyper-eutrophic subtropical lagoon. J. Environ. Sci. Health A Tox. Hazard. Subst. Environ. Eng. 49 (1), 116–124.

Lacroix, R., Robert, S., Poncelet, P., Kasthuri, R.S., Key, N.S., Dignat-George, F., et al., 2010 Nov. Standardization of platelet-derived microparticle enumeration by flow cytometry with calibrated beads: results of the International Society on Thrombosis and Haemostasis SSC Collaborative workshop. J. Thromb. Haemost. 8 (11), 2571–2574.

Lai, M.C., Shu, C.M., Chen, S.C., Lai, L.J., Chiou, M.S., Hua, J.J., 2000 Jul. Methanosarcina mazei strain O1M9704, methanogen with novel tubule isolated from estuarine environment. Curr. Microbiol. 41 (1), 15–20.

Lapinski, M.M., Castro-Forero, A., Greiner, A.J., Ofoli, R.Y., Blanchard, G.J., 2007 Nov 6. Comparison of liposomes formed by sonication and extrusion: rotational and translational diffusion of an embedded chromophore. Langmuir 23 (23), 11677–11683.

Lazaro-Ibanez, E., Sanz-Garcia, A., Visakorpi, T., Escobedo-Lucea, C., Siljander, P., Ayuso-Sacido, A., et al., 2014 Oct. Different gDNA content in the subpopulations of prostate cancer extracellular vesicles: apoptotic bodies, microvesicles, and exosomes. Prostate 74 (14), 1379–1390.

Lee, K., Shao, H., Weissleder, R., Lee, H., 2015 Mar 24. Acoustic purification of extracellular microvesicles. ACS Nano 9 (3), 2321–2327.

Li, Z., Clarke, A.J., Beveridge, T.J., 1998 Oct. Gram-negative bacteria produce membrane vesicles which are capable of killing other bacteria. J. Bacteriol. 180 (20), 5478–5483.

Lin, G.S., Macey, R.I., 1978 Sep 22. Shape and stability changes in human erythrocyte membranes induced by metal cations. Biochim. Biophys. Acta 512 (2), 270–283.

Maas, S.L., de Vrij, J., van der Vlist, E.J., Geragousian, B., van Bloois, L., Mastrobattista, E., et al., 2015 Feb 28. Possibilities and limitations of current technologies for quantification of biological extracellular vesicles and synthetic mimics. J. Control. Release 200, 87–96.

Machida, K., Imataka, H., 2015 Apr. Production methods for viral particles. Biotechnol. Lett. 37 (4), 753–760.

Marchesi, V.T., Palade, G.E., 1967 Nov. The localization of Mg–Na–K-activated adenosine triphosphatase on red cell ghost membranes. J. Cell Biol. 35 (2), 385–404.

Matsuzaki, K., Murase, O., Sugishita, K., Yoneyama, S., Akada, K., Ueha, M., et al., 2000 Jul 31. Optical characterization of liposomes by right angle light scattering and turbidity measurement. Biochim. Biophys. Acta 1467 (1), 219–226.

McFarlane, C., Young, I.S., Hare, L., Mahon, G., McEneny, J., 2005 Mar. A rapid methodology for the isolation of intermediate-density lipoprotein: characterization of lipid composition and apoprotein content. Clin. Chim. Acta 353 (1-2), 117–125.

Nicolet, A., Meli, F., Evd, P., Yuana, Y., Gollwitzer, C., Krumrey, M., et al., 2016. Inter-laboratory comparison on the size and stability of monodisperse and bimodal synthetic reference particles for standardization of extracellular vesicle measurements. Meas. Sci. Technol. 27 (3), 035701.

Okutucu, B., Dincer, A., Habib, O., Zihnioglu, F., 2007 Aug 1. Comparison of five methods for determination of total plasma protein concentration. J. Biochem. Biophys. Methods 70 (5), 709–711.

Osburn, M.R., Amend, J.P., 2011 Jan. *Thermogladius shockii* gen. nov., sp. nov., a hyperthermophilic crenarchaeote from Yellowstone National Park, USA. Arch. Microbiol. 193 (1), 45–52.

Oster, G., 1950 May 20. Two-phase formation in solutions of tobacco mosaic virus and the problem of long-range forces. J. Gen. Physiol. 33 (5), 445–473.

Perusse, M., Pascot, A., Despres, J.P., Couillard, C., Lamarche, B., 2001 Aug. A new method for HDL particle sizing by polyacrylamide gradient gel electrophoresis using whole plasma. J. Lipid Res. 42 (8), 1331–1334.

Petersen, K.E., Manangon, E., Hood, J.L., Wickline, S.A., Fernandez, D.P., Johnson, W.P., et al., 2014 Dec. A review of exosome separation techniques and characterization of B16-F10 mouse melanoma exosomes with AF4-UV-MALS-DLS-TEM. Anal. Bioanal. Chem. 406 (30), 7855–7866.

Salpeter, M.M., Zilversmit, D.B., 1968 Mar. The surface coat of chylomicrons: electron microscopy. J. Lipid Res. 9 (2), 187–192.
Samuel, M., Bleackley, M., Anderson, M., Mathivanan, S., 2015 Sep 23. Extracellular vesicles including exosomes in cross kingdom regulation: a viewpoint from plant–fungal interactions. Front. Plant Sci. 6, 766.
Santi, L., Huang, Z., Mason, H., 2006 Sep. Virus-like particles production in green plants. Methods 40 (1), 66–76.
Sawle, A., Higgins, M.K., Olivant, M.P., Higgins, J.A., 2002 Feb. A rapid single-step centrifugation method for determination of HDL, LDL, and VLDL cholesterol, and TG, and identification of predominant LDL subclass. J. Lipid Res. 43 (2), 335–343.
Schooling, S.R., Beveridge, T.J., 2006 Aug. Membrane vesicles: an overlooked component of the matrices of biofilms. J. Bacteriol. 188 (16), 5945–5957.
Spinrad, R.W., Brown, J.F., 1986 Jun 15. Relative real refractive index of marine microorganisms: a technique for flow cytometric estimation. Appl. Opt. 25 (12), 1930.
Tatischeff, I., Larquet, E., Falcon-Perez, J.M., Turpin, P.Y., Kruglik, S.G., 2012 Nov 21. Fast characterisation of cell-derived extracellular vesicles by nanoparticles tracking analysis, cryo-electron microscopy, and Raman tweezers microspectroscopy. J. Extracell Vesicles 1. http://dx.doi.org/10.3402/jev.v1i0.19179 (eCollection 2012).
van Antwerpen, R., La Belle, M., Navratilova, E., Krauss, R.M., 1999 Oct. Structural heterogeneity of apoB-containing serum lipoproteins visualized using cryo-electron microscopy. J. Lipid Res. 40 (10), 1827–1836.
van der Meel, R., Fens, M.H., Vader, P., van Solinge, W.W., Eniola-Adefeso, O., Schiffelers, R.M., 2014 Dec 10. Extracellular vesicles as drug delivery systems: lessons from the liposome field. J. Control. Release 195, 72–85.
van der Pol, E., van Gemert, M.J., Sturk, A., Nieuwland, R., van Leeuwen, T.G., 2012 May. Single vs. swarm detection of microparticles and exosomes by flow cytometry. J. Thromb. Haemost. 10 (5), 919–930.
van der Pol, E., Coumans, F.A., Grootemaat, A.E., Gardiner, C., Sargent, I.L., Harrison, P., et al., 2014 May 13a. Particle size distribution of exosomes and microvesicles determined by transmission electron microscopy, flow cytometry, nanoparticle tracking analysis, and resistive pulse sensing. J. Thromb. Haemost.
van der Pol, E., Coumans, F.A., Sturk, A., Nieuwland, R., van Leeuwen, T.G., 2014 Oct 2b. Refractive index determination of nanoparticles in suspension using nanoparticle tracking analysis. Nano Lett.
van der Pol, E., Boing, A.N., Gool, E.L., Nieuwland, R., 2016 Jan. Recent developments in the nomenclature, presence, isolation, detection and clinical impact of extracellular vesicles. J. Thromb. Haemost. 14 (1), 48–56.
Varga, Z., Yuana, Y., Grootemaat, A.E., van der Pol, E., Gollwitzer, C., Krumrey, M., et al., 2014 Feb 4. Towards traceable size determination of extracellular vesicles. J. Extracell Vesicles 3. http://dx.doi.org/10.3402/jev.v3.23298 (eCollection 2014).
Virtanen, J.A., Cheng, K.H., Somerharju, P., 1998 Apr 28. Phospholipid composition of the mammalian red cell membrane can be rationalized by a superlattice model. Proc. Natl. Acad. Sci. U. S. A. 95 (9), 4964–4969.
Wang, L., Zhao, W., Tan, W., 2008. Bioconjugated silica nanoparticles: development and applications. Nano Res. 1 (2), 99–115.
Wood, R.J., Volek, J.S., Liu, Y., Shachter, N.S., Contois, J.H., Fernandez, M.L., 2006 Feb. Carbohydrate restriction alters lipoprotein metabolism by modifying VLDL, LDL, and HDL subfraction distribution and size in overweight men. J. Nutr. 136 (2), 384–389.
Yanez-Mo, M., Siljander, P.R., Andreu, Z., Zavec, A.B., Borras, F.E., Buzas, E.I., et al., 2015 May 14. Biological properties of extracellular vesicles and their physiological functions. J. Extracell Vesicles 4, 27066.
Yoon, J., Jo, W., Jeong, D., Kim, J., Jeong, H., Park, J., 2015 Aug. Generation of nanovesicles with sliced cellular membrane fragments for exogenous material delivery. Biomaterials 59, 12–20.
Yoshioka, Y., Konishi, Y., Kosaka, N., Katsuda, T., Kato, T., Ochiya, T., 2013 Jun 18. Comparative marker analysis of extracellular vesicles in different human cancer types. J. Extracell. Vesicles 2. http://dx.doi.org/10.3402/jev.v2i0.20424 (eCollection 2013).
Zinsser, H., Tang, F.F., 1927 Jul 31. Studies in ultrafiltration. J. Exp. Med. 46 (2), 357–378.